Synthesis and Characterization of Poly(fluorinated acrylate)/Silica Hybrid Nanocomposites

Li Yao, Tingting Yang, Shiyuan Cheng

School of Materials Science and Engineering, Hubei University, Wuhan 430062, People's Republic of China

Received 13 July 2007; accepted 25 March 2009
DOI 10.1002/app.30526
Published online 4 November 2009 in Wiley InterScience (www.interscience.wiley.com).

ABSTRACT: The nanocomposite particles (NPs) with inorganic silica as core and fluorinated polymer shell have been *in situ* synthesized via emulsion polymerization. The chemical composition and core-shell structure were characterized by Fourier-transform infrared spectrometry and transmission electron microscopy. The results showed that silica nanoparticles were encapsulated in latex particles, with single- and multicore morphologies coexisting. Thermal gravimetric analysis also suggested the successful encapsulation of silica into NPs with enhanced thermal stability. The surface properties of the latex films produced from the core-shell particles were also investigated by contact angle method and water absorption measurement. Both fluorinated polymer and silica contributed to less water absorption ratio and lower surface-free energy, which was composed of larger polar component and smaller disperse component, just reversed as usual.
 J Appl Polym Sci 115: 3500–3507, 2010

Key words: silica; poly(fluorinated acrylate); emulsion polymerization; surface-free energy; nanocomposites

INTRODUCTION

In the past decade, organic–inorganic nanocomposites have attracted a great deal of interest from material scientists because of their extraordinary properties deriving from the synergism between each individual component.[1–5] Actually, the combination of inorganic and organic components at the nanosize level in a single material has made accessible an immense new area of materials science, because this combination can dramatically improve material properties in engineering plastics, enhanced rubber, coatings and adhesives.

The effects of different nanoparticles on the properties of polymers vary depending on the composition and microstructure. When F-containing entities are incorporated into the structure of polyacrylate, some properties are improved (e.g., oil and water repellency, refraction index, dielectric constant, and thermal resistance).[6–9] Therefore, poly(fluorinated acrylate) (PFA) has attracted much attention for applications in surface coatings, optical communication, microelectronics, and medicine.[10–12] As an inexpensive functional component, incorporated silica can shield polymeric matrix from ultraviolet rays, while reinforcement and improved thermal stability can be achieved as well as better rinse-resistance, perdurability, and self-cleanness effects.[13,14]

Correspondence to: S. Cheng (scheng@public.wh.hb.cn).

Journal of Applied Polymer Science, Vol. 115, 3500–3507 (2010)

Research on organic–inorganic hybrid materials was widely reported in the literature. Usually, sol–gel method was applied to prepare organic–inorganic hybrids, and there have been a variety of such studies on the organic polymers/silica hybrids in which silica were dispersed in polymeric matrix.[15,16] However, the preparation of fluorinated polymer hybrids is very limited except for some reports on the synthesis of poly(methacrylic acid)/TEOS/2-perfluorooctylethyl-triethoxysilane polymer hybrids, poly(vinylidene fluoride)/SiO_2 hybrid composites,[17,18] fluorinated polyimides,[19] telechelic perfluoropolyethers-containing triblock copolymers,[20] and Nafion^{TR} resin/silica composites,[21] etc. Moreover, the usage of large amount of solvent in sol–gel method is unfriendly to environment, and time-consuming posttreatment of solvent is also needed. Another strategy to synthesize hybrid fluorinated polymer is based on polymerization involving organosilicon monomers and fluorinated monomers,[22–24] but its application is greatly restricted due to the high price of these functionalized monomers. As controlled radical polymerization technique emerged, polymers with well-controlled molecular weights, narrow molecular weight distributions, and desired architecture from a wide range of conjugated vinyl monomers can be prepared.[25] It may be a good approach to combine silica and fluorinated polymer with well-defined polymer chains grafted on silica, but it is also a costly and complicated process.

Emulsion polymerization, one of the most important methods, can produce not only organic–

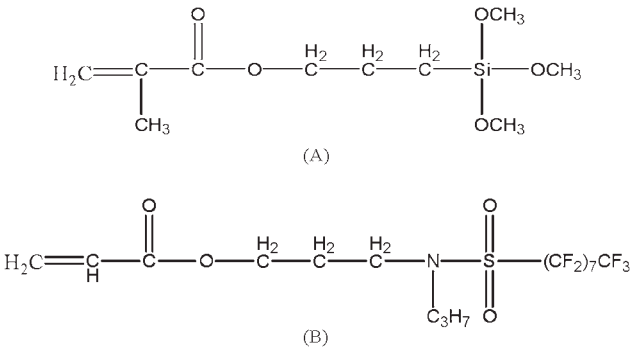

Scheme 1 Molecular structures of chemical components involved in the synthesis of silica/PFA NPs: (A) MPS, (B) FA.

inorganic hybrids but also environment friendly fluoropolymers. So far, there is little literature reporting direct-introduction of silica into fluorinated polymer via emulsion polymerization, which was simply embedded and only weak bonds, mainly hydrogen bonds, were present at the interface.[26–29] To strengthen the interaction of the two phases, adding a small amount of coupling agents is an effective method,[30] as well as promoting synergistic effects. There is lacking in reports about combining silica- and fluorine-containing polymer with covalent bonds via emulsion polymerization, which provides the two phases a more intimate cooperation.

In this context, silica/PFA nanocomposites with core-shell structure were obtained via emulsion polymerization, where γ-methacryloxypropyl trimethoxysilane (MPS) was utilized to strengthen interactions between polymer and silica. Fourier transform infrared spectrometry (FTIR), transmission electron microscopy (TEM), and thermal gravimetric analysis (TGA) have been used to characterize the chemical composition, morphology, and property of PFA/silica nanocomposites. Additionally, the effects of silica and FA contents on the surface properties of latex films have been also investigated.

MATERIALS AND METHODS

Materials

Tetraethoxysilane (TEOS) (C.R.), ammonia (25% in water), and absolute ethanol (A.R.) (Shanghai Zhenxin Chemicals Co. Ltd., Shanghai, China), were used as received. MPS (A.R.), with molecular structure shown in Scheme 1(A), was acquired from Aldrich and used as received.

2-(*N*-propylperfluorooctanesulfonamido) ethyl acrylate (FA) was prepared as reported,[31] with formula as Scheme 1(B) demonstrates.

The monomers, methyl methacrylate (MMA) and butyl acrylate (*n*-BA) (A.R.), purchased from Tianjin Bodi Chemicals, were treated with 1*M* NaOH aqueous solutions to remove the inhibitor before usage. Initiator, ammonium persulfate (APS) (A.R.), was purified by recrystallization. Emulsifiers, sodium dodecyl benzene sulfonate (SDBS) (A.R.) and OS-15 (C.P.), were used without further purification (Shanghai Yingpeng Chemicals Co. Ltd., Shanghai, China). Deionized water was applied throughout all polymerization and treatment processes.

Synthetic procedure

The monodisperse silica nanoparticles were prepared in ethanol according to the well-known Stöber procedure.[32] The functionalization of the silica was carried out by adding MPS directly into the dispersion of silica nanoparticles in ethanol under vigorous machine stirring. After the mixture was stirred overnight at ambient temperature, the mixture was held at 80°C for 1.5 h to promote covalent bonding of the organosilane to the surface of the silica nanoparticles. The MPS-grafted silica suspensions were then dialyzed against water until neutral pH to remove the remaining reactants and replace ethanol with water. If necessary, the silica suspensions were concentrated and their final concentration was determined by measuring the mass of a dried extract. Silica particle sizes were determined statistically while analyzing TEM pictures. Due to an excessive amount of silica and a small amount of MPS, a nearly complete conversion of MPS can be achieved, so the MPS-grafted density of silica nanoparticles can be determinate as follows:

$$\text{MPS-grafted density of } SiO_2\ (\text{mol/m}^2) = \frac{\frac{\rho(\text{MPS})\times V(\text{MPS})}{M(\text{MPS})}}{\frac{\frac{\rho(\text{TEOS})\times V(\text{TEOS})}{M(\text{TEOS})}\times M(SiO_2)}{\rho(SiO_2)\times V(SiO_2)}} \times S(SiO_2)$$

where ρ, *M*, *V*, and *S* designate the density, the molar mass, the surface area, and the volume of compound, respectively.

PFA/silica NPs were synthesized by emulsion polymerization in the presence of silica particles, which was carried out in a 250-mL four-necked flask equipped with a mechanical stirrer, thermometer, and condenser. Required amounts of surfactants and silica suspensions were introduced into the reaction flask containing distilled water under stirring for 30 min in a nitrogen atmosphere. Then the temperature was raised to 40°C and monomers were charged. It was stirred another 30 min, followed by the addition of APS to initiate the polymerization at 70°C. The reaction was then allowed to polymerize for 4 h to achieve a higher conversion and was cooled to room temperature and pH adjusted to 7 with ammonia. The detailed recipes of the prepared samples are listed in Table I.

TABLE I
Recipes for Preparation of Silica/PFA NPs

		Monomers			Surfactants				
Sample no.	Silica (g)	FA (g)	*n*-BA (g)	MMA (g)	SDBS (g)	OS-15 (g)	APS (g)	DI water (g)	Conversion (%)
1	0	0	5.0	5.0	0.1	0.1	0.05	75	99.14
2	0.2	0	5.0	5.0	0.1	0.1	0.05	75	98.88
3	0.2	0.25	5.0	5.0	0.1	0.1	0.05	75	98.25
4	0.2	0.5	5.0	5.0	0.1	0.1	0.05	75	97.92
5	0.2	1.0	5.0	5.0	0.1	0.1	0.05	75	98.49
6	0.2	1.5	5.0	5.0	0.1	0.1	0.05	75	95.80
7	0	0.25	5.0	5.0	0.1	0.1	0.05	75	98.76
8	0.1	0.25	5.0	5.0	0.1	0.1	0.05	75	99.21
9	0.4	0.25	5.0	5.0	0.1	0.1	0.05	75	98.30
10	0.6	0.25	5.0	5.0	0.1	0.1	0.05	75	97.08
11	0.8	0.25	5.0	5.0	0.1	0.1	0.05	75	91.53
12	0.2[a]	0.25	5.0	5.0	0.1	0.1	0.05	75	99.56

[a] Silica without MPS-modified.

Characterization

FTIR spectra of the latex films were measured in the range from 4000 to 450 cm^{-1} with a Perkin-Elmer Spectrum One FTIR spectrometer.

The morphologies of the silica and latex particles were investigated by TEM. The silica suspensions were diluted directly, while the latices were diluted and then stained with a phosphotungstic acid solution (pH 6.4). TEM experiments were performed with a TEX-100SX microscope (Japan, accelerating voltage of 80 kV). The samples were prepared as follows: silica nanoparticles and silica/PFA NPs were dispersed in water and one drop of the dilute suspension was deposited on a copper grid coated with a carbon membrane.

To examine the thermal stability of silica/PFA films prepared, the thermal decomposition temperature of nanocomposites was measured with a Perkin-Elmer TGA7 thermogravimeter, under a nitrogen atmosphere at a heating rate of 20°C/min.

Weighed latex films [$2.0 \times 1.5 \times (0.6 \pm 0.1)$ cm^3] were dipped in distilled water for 72 h. Then, the water on the surface of the films was removed, and the films were weighed again. The water absorption ratio of silica/PFA films was calculated with the following formula: water absorption ratio (wt %) = $(W_1 - W_0)/W_0 \times 100\%$, where W_0 and W_1 are the weights of the films before and after the films absorb water, respectively. To receive an exact result, five samples were measured parallelly.

The dynamic contact angles of the latex films were measured by the Wilhelmy method at 25°C with a Krüss II interface tension meter (Krüss GmbH, Hamburg, Germany). The latex films were cut into squares, held in a microbalance, progressively immersed in different liquids at a speed of 0.5 mm/s, and then conversely receded to the original position. An analysis of the wetting force data yielded both an advancing contact angle and a receding contact angle. Considering advancing contact angles for different liquids, the surface tension can be calculated by the following equation[33]:

$$\gamma_{\text{solid}} = \gamma^d_{\text{solid}} + \gamma^p_{\text{solid}}$$

$$\gamma_{\text{liquid}}(\cos\theta + 1) = 2\left(\gamma^d_{\text{solid}}\gamma^d_{\text{liquid}}\right)^{1/2} + 2\left(\gamma^p_{\text{solid}}\gamma^p_{\text{liquid}}\right)^{1/2}$$

where is the surface-free energy and the superscripts d and p correspond to dispersion and polar components of the surface-free energy, respectively. The wetting liquids used for contact angles measurements were water and diiodomethane, as Owens and Wendt suggested,[34] wherein γ, γ^d, and γ^p of water are 72.8, 21.8, and 51.0 mN/m and of diiodomethane are 50.8, 48.5, and 2.3 mN/m.

RESULTS AND DISCUSSION

Preparation of silica and grafted silica nanoparticles

Silica nanoparticles were synthesized from TEOS with absolute ethanol as a solvent medium, that is, a sol–gel process. Silica nanoparticles grew at a very slow rate, and a long time (usually 24 h) was required to produce uniform nanosized particles well under control. The appearance of the silica nanoparticles dispersive solution during the course of the reaction showed that with elapsed reaction time, silica nanoparticles grew gradually. The dispersive solution was transparent initially, but turned weak blue later. Figure 1(A) shows the TEM image of the silica nanoparticles with an average diameter of 18 nm, obtained by calculating the diameter from

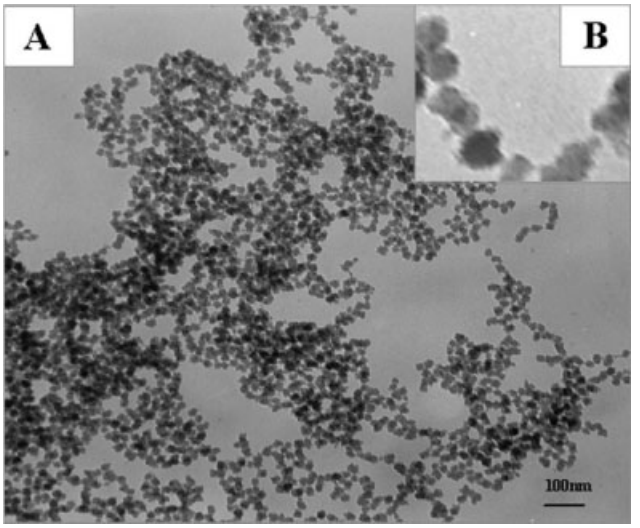

Figure 1 TEM images of (A) silica nanoparticles and (B) a five-times-magnified image of silica nanoparticles.

the TEM image. To distinctly observe the unsmooth morphology, we selected a part of the TEM image and magnified it five times, as shown in Figure 1(B). The surface of the silica nanoparticles consists of many hydroxyl groups, resulting in significant interactions between the surface of the silica nanoparticles and H_2O. Therefore the surface of the silica nanoparticles is not ideal spherical and unsmooth.

To improve the interfacial adhesion between the silica nanoparticles and PFA molecules, silane-coupling agents have formerly been used on the silica.[35] At the interface, the hydroxyl group of silanes and silanol groups of nanosilica surface can react with each other through siloxane bonding or hydrogen bonding, which indicated the graft process of silane-coupling agents onto silica nanoparticles. FTIR spectroscopy offers qualitative information on the way in which the silane-coupling agent is bound to the surface of silica nanoparticles. The FTIR spectra of silica nanoparticles before and after modification are shown in Figure 2. Both spectrum before and after modification show intensive bands in the vicinity of 1090 and 474 cm^{-1} related to Si—O—Si vibrations, which are characteristic of silica nanoparticles. The broad band at 3450 cm^{-1} is attributed to hydroxyl group on the surface, and three adsorption bands at 1646 (SiO—H bending),[36] 970, and 801 cm^{-1} indicate adsorbed molecular water in the sample.[37] As expected, absorption bands characteristic of the Si—O—C group at 1100 cm^{-1}, as well as 2979 and 1722 cm^{-1} corresponding to the stretching vibration of the —CH_3 and C=O groups, appear in spectrum after modification [Fig. 2(B)], which verify the presence of MPS. However, the unattached MPS in the MPS-modified particles was thoroughly removed before the FTIR test; as described in the previous section, these typical MPS bands demonstrate that the coupling agent MPS was indeed attached to the surface of the silica nanoparticles via chemical bonds. According to the amount of MPS added, the MPS-grafted density of silica nanoparticles was calculated to be 0.1716 μmol/m^2. Correspondingly, the absorption band at 3439 cm^{-1} refers to the remaining hydroxyl group, with a faintly reduced strength. Then the grafted silica nanoparticles were used as cores in the encapsulation polymerization.

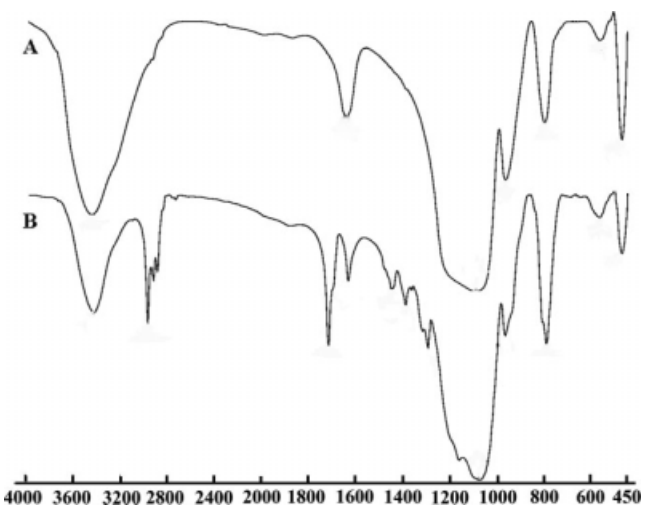

Figure 2 FTIR spectra of (A) silica; (B) MPS-grafted silica.

Preparation of silica/PFA core-shell microspheres

Silica/PFA core-shell microspheres were obtained through *in situ* emulsion polymerization of MMA, BA, and FA, in which process MPS-grafted silica

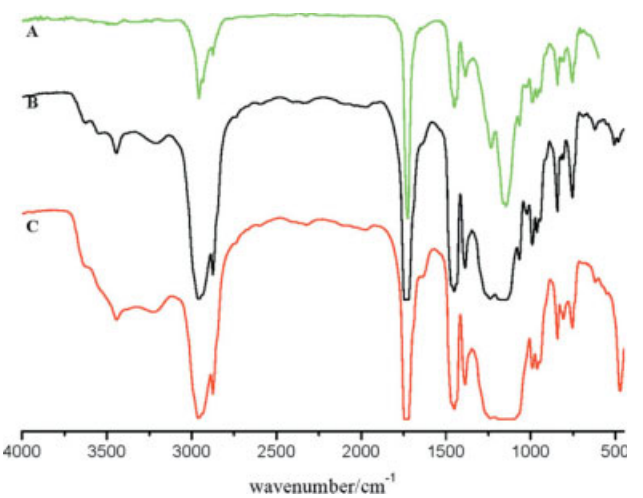

Figure 3 FTIR spectra of (A) Sample 1, (B) Sample 7, and (C) Sample 3. [Color figure can be viewed in the online issue, which is available at www.interscience.wiley.com.]

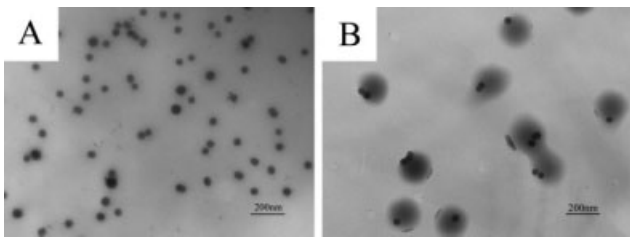

Figure 4 TEM images of (A) Sample 12 and (B) Sample 3.

were used as seeds. The chemical structure of nanosilica/polyacrylate composite latex was measured by FTIR spectroscopy. Figure 3 shows the FTIR spectra of poly (MMA-*co*-BA), PFA, and silica/PFA core-shell microspheres. The characteristic absorption of the C=C bond at 1640 cm^{-1} disappears, indicating that monomers are polymerized. Absorption bands at 1100–1289 cm^{-1} related to the C—F group and 1250 cm^{-1} related to the C—O—C in the PFA chains[38] overlap, as shown in Figure 3(B). It is wide and blunter and could not be clearly distinguished. The absorption bands at 1108 cm^{-1} (asymmetric Si—O stretching vibration) and 474 cm^{-1} (Si—O—Si bending vibration),[39] which only appear in Figure 3(C), indicate that the silica nanoparticles are doped in the polymer. It is noteworthy that the tether between the silica (Si—O—Si 1108 cm^{-1}) and PFA chains make those band absorptions more significantly superposed, shown as a wider absorption band range from 1050 to 1300 cm^{-1} in Figure 3(C).

Figure 4 are TEM images of resulting silica/PFA latex particles with unmodified and modified silica nanoparticles as seeds. While using unmodified silica particles (Sample 12), PFA mostly self-nucleates and propagates to form pure PFA particles but did not graft on the surface of silica nanoparticles, so silica nanoparticles are separated one from another by matrix of PFA, as shown in Figure 4(A). In contrast, after the modification of silica by MPS, acrylate monomers are grafted from the particle surface to carry out the polymerization. Thus, PFA is grafted on the surface of silica nanoparticles and forms the silica/PFA NPs. Therefore, the resulting latex particles have a uniform size (Sample 3), as seen in Figure 4(B). Clearly, MPS-grafted silica acts as seeds in the reaction. The spherical particles show obvious core-shell structures; light PFA shells coat the dark grafted silica core spheres, and approximately 50% of these core-shell microspheres have more than one single core, which is due to the congregating of smaller particles when the diameters of the core are not larger than 100 nm. The average diameters of the monodisperse core-shell microspheres vary from 170 to 190 nm. It is noticeable that all the silica cores are off-center. The reason is that the MPS-grafted density of silica is the key of the morphology of latex particles obtained.[40,41] Herein, under a low MPS-grafted density, not all of monomers are polymerized and connected with MPS on the grafted silica, and most of the polymer chains are twisted and absorbed around the core particles, resulting in an off-center core-shell structure ultimately.

Thermal stability of latex films

The thermal decomposition behavior of the silica/PFA samples with different silica contents were investigated by TGA at a heating rate of 20°C/min under a nitrogen flow, as illustrated in Figure 5, which reveals two principal thermal events occurring in the following temperature zone: room temperature to 240°C and 240–800°C. The first zone can be attributed to the loss of adsorbed water, while the second weight loss corresponds to the decomposition of fluorinated polyacrylate. Obviously, we can see a raise of about 5.1°C of the initiative decomposition temperature as silica are incorporated into PFA, which also verifies the successful incorporation of silica into NPs. Furthermore, the silica contents of silica/PFA samples are determined from the weight loss of samples at 800°C. The final residue weight of silica/PFA NPs after at 800°C is 3.6% in Figure 5(b) (Sample 9) and 7.1% in Figure 5(c) (Sample 11), respectively, which suggest that the silica content of the NPs samples increases from 3.6 to 7.1%, while the amount of grafted silica rise from 0.4 to 0.8 g. In fact, silica incorporated act as crosslinking. With more silica introduced, the crosslinkage of PFA increases, and the thermal stability of samples is enhanced. The initiative and maximum-rate decomposition temperature both raise nearly 8.2°C, while silica content increase from 3.6 to 7.1%.

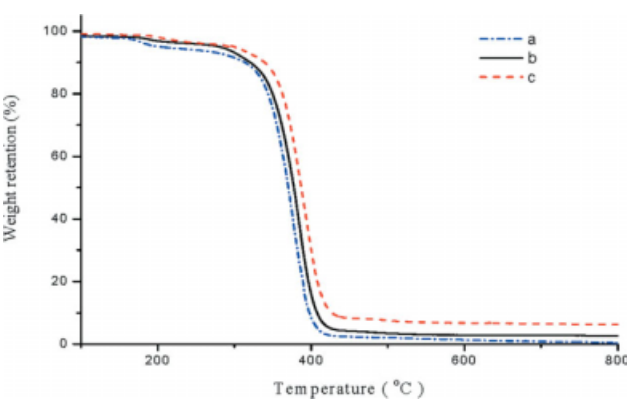

Figure 5 TGA curves of (a) Sample 1, (b) Sample 9, and (c) Sample 11. [Color figure can be viewed in the online issue, which is available at www.interscience.wiley.com.]

TABLE II
Contact Angle, Surface-Free Energy, and Water Absorption Ratio of Latex Films with Different FA Contents

Sample no.	Contact angle (°)		Surface-free energy (mN/m)			Water absorption ratio (wt %)
	Water	Diiodomethane	γ	γ^d	γ^p	
1	61.2	72.1	40.0	13.3	26.7	37.86
2	74.3	76.0	30.0	13.2	16.8	28.14
3	91.6	93.1	17.5	7.6	9.9	14.76
4	97.0	98.1	14.3	6.3	8.0	10.59
5	103.9	107.2	10.6	4.0	6.5	9.86
6	105.4	111.3	9.8	3.1	6.7	12.27

Surface properties of latex films

The contact angle has commonly been used as a criterion for the evaluation of hydrophobic surfaces. Usually an increased contact angle indicated an increased hydrophobicity. The fluorinated polymer has low surface-free energy property, and incorporation of fluorinated moieties into a polymer has been shown to be effective for the enhancement of the hydrophobicity of film's surface. As shown in Table II, the water contact angles on the latex film containing more than 2.0 wt % FA (vs. MMA and *n*-BA) are all above 90°, with surface-free energy less than 20 mN/m, suggesting that even a small amount of FA introduced contributes to hydrophobic property. The more FA the latex films contain, the larger contact angles are. Besides, the diiodomethane contact angles of latex films showed a similar trend. The surface-free energy (γ) and its dispersion (γ^d), polar components (γ^p), are calculated from the contact angles of water and diiodomethane, by extended Fowkes equation; the results are listed in Table II. The surface-free energies of films containing fluorine are much lower than those without fluorine. The surface-free energy and dispersion, polar components, all decreased with increasing FA content. It is noticeable that the extent of contact angles increasing slows down as FA increases at a constant rate, probably as a result of two reasons. On the one hand, as more and more FA are added, nearly fully coverage of perfluoroalkyl is achieved on the film surfaces, and contact angles approach the maximum; on the other hand, due to the hydrophobic and oleophobic properties of FA, it is more difficult to enter micelles especially at a high concentration of FA, thus the copolymeric efficiency of FA decreases while the total amount of FA increases. What is worth noting is the abnormal γ^d and γ^p of latex films. Generally, larger γ^d and less γ^p constitute surface-free energy,[42] but the exact opposite is true. It may be attributed to the silica introduced, which lay on the edge of silica/PFA NPs in the TEM images, and conduces a different morphology while film-forming. Silica particles existing on the surface may to some extent confine the migration of fluorinated polymer chains,[27] which also contributes to the abnormal γ^d and γ^p. The phenomena are still under further investigation.

The data in Table II also reveal the effects of FA on the water absorption ratio of the latex films. FA lying in the shell partly immigrate to the surface while film forming, so the more FA in the latex film, the more perfluoroalkyl groups concentrate on the film surface, even after the films are immersed in water. Thus, sufficient amounts of strongly hydrophilic perfluoroalkyl groups on the film surface

TABLE III
Contact Angle, Surface-Free Energy, and Water Absorption Ratio of Latex Films with Different Silica Contents

Sample no.	Contact angle (°)		Surface-free energy (mN/m)			Water absorption ratio (wt %)
	Water	Diiodomethane	γ	γ^d	γ^p	
1	61.2	72.1	40.0	13.3	26.7	37.86
7	82.9	87.8	23.1	8.8	14.4	23.21
8	86.8	93.7	20.3	6.8	13.5	18.77
3	91.6	93.1	17.5	7.6	9.9	14.76
9	91.4	92.7	17.7	7.8	9.9	14.77
10	91.5	93.2	17.6	7.6	10.0	14.55
11	87.5	88.7	20.3	9.0	11.3	17.88
12	88.9	92.5	19.1	7.6	11.5	16.39

prohibit water molecules from penetrating into the inner parts of latex films and enhance the water resistance of the films, hence, water absorption decreases. However, there is something exceptional, namely, water absorption increases, while FA content increases to 15.0 wt %.

Surface properties of latex films with different silica content were studied similarly. From Table III, the introduction of silica improves the surface properties of latex films. The general tendency is the surface-free energy decreases with increasing silica content, and the hydrophobic property is enhanced at the same time. There may be several reasons. First, the crosslinkage of PFA increases because of the silica introduced. On the one hand, polymer chains that twist on the surface of silica induce physical crosslinking; on the other hand, MPS that graft on the silica surface copolymerizes with acrylate monomers result in chemical crosslinking. Second, the hydrophobic effects exist because of the Si—O—Si bonds and partly organosilicone-substituted —OH group at silica surface. Third, the incorporation of silica acts as protuberance on the surface of latex films because PFA of relatively low glass-transition temperature amalgamates, resulting in the increase of the surface roughness and the decrease of surface-free energy. Thus, the larger contact angle for water and lower water absorption ratio are presented, while more silica was contained in the latex films. However, the tendency slows down to be plateau-like, while the silica content exceeded 2.0 wt % (vs. MMA and *n*-BA); and if silica content exceeds 6.0 wt %, the polymerization stability is brought down and gels are produced. Both partial FA and silica were coagulated from the emulsion system, leading to lower water contact angle and larger water absorption ratio.

Compared with Sample 12, Sample 3 with MPS-grafted silica encapsulated had a lower surface-free energy. Because the hydroxyl group on the surface of silica are substituted by the alkylene in MPS, which take part in copolymerization later, the number of hydrophilic group (mainly —OH) on the surface slightly decreases, as well as physical and chemical crosslinkage, bringing on a lower surface-free energy and less water absorption ratio.

CONCLUSION

The silica/PFA latex had been successfully prepared by emulsion polymerization at the present of silica. TEM images effectively demonstrate the formation of the silica/PFA core-shell structure. Encapsulated silica enhances thermal stability of NPs, which is confirmed by TGA. Through analyzing the surface properties of the latex films via contact angle and water absorption measurements, we can see that excellent water and oil repellency can be achieved. Both silica and fluorinated component incorporated to contribute to the decrease of surface-free energy, which is composed of abnormal polar and disperse components.

References

1. Huynh, W. U.; Dittmer, J. J.; Alivisatos, A. P. Science 2002, 295, 2425.
2. Tessler, N.; Medveder, V.; Kazes, M.; Kan, S. H.; Banin, U. Science 2002, 295, 1506.
3. Lee, L. H.; Chen, W. C. Chem Mater 2001, 11, 1137.
4. Lin, W. J.; Chen, W. C.; Wu, W. C.; Niu, Y. H.; Jen, A. K.-Y. Macromolecules 2004, 37, 2335.
5. Wang, Y. W.; Yen, C. T.; Chen, W. C. Polymer 2005, 46, 6959.
6. Yang, S.; Wang, J.; Ogino, K.; Valiyaveettil, S.; Ober, C. K. Chem Mater 2000, 12, 33.
7. Lee, J. R.; Jin, F. L.; Park, S. J.; Park, J. M. Surf Coat Technol 2004, 180, 650.
8. Ravenstein, L.; Ming, W.; Grampel, R. D.; Linde, R.; With, G.; Loontjens, T.; Thüne, P. C.; Niemantsverdriet, J. M. Macromolecules 2004, 37, 408.
9. Wei, H. M.; Luc, V. R.; Robert, V. D. G. Polym Bull 2001, 47, 321.
10. Riess, J. G. J Fluorine Chem 2002, 114, 119.
11. Lowe, K. C. J Fluorine Chem 2001, 109, 59.
12. Krafft, M. P. Adv Drug Delivery Rev 2001, 47, 209.
13. Fabbri, P.; Singh, B.; Leterrier, Y.; Månson, J. A. E.; Messori, M.; Pilati, F. Surf Coat Technol 2006, 200, 6706.
14. Zhang, K.; Ma, J.; Zhang, B.; Zhao, S.; Li, Y. P.; Xu, Y. X.; Yu, W. Z.; Wang, J. Y. Mater Lett 2007, 61, 949.
15. Novak, B. M. Adv Mater 1993, 5, 422.
16. Wen, J.; Wilkes, G. L. Chem Mater 1996, 8, 1667.
17. Ogoshi, T.; Chujo, Y. J Polym Sci Part A: Polym Chem 2005, 43, 3543.
18. Kim, D. S.; Park, H. B.; Lee, Y. M.; Park, Y. H.; Rhim, J. W. J Appl Polym Sci 2004, 93, 209.
19. Cornelius, C. J.; Marand, E. Polymer 2002, 43, 2385.
20. Messori, M.; Toselli, M.; Pilati, F.; Mascia, L.; Tonelli, C. Eur Polym J 2002, 38, 1129.
21. Harmer, M. A.; Farneth, W. E.; Sun, Q. J Am Chem Soc 1996, 118, 7708.
22. Wu, W. L.; Ni, Y. R.; Liao, J. F.; Gan, K. M.; Ye, J. C. Guangzhou Chem Ind Technol 2005, 33, 30.
23. Huang, Y. W.; Liu, W. Q.; Kou, Y.; Luo, G. J. Polym Mater Sci Eng 2006, 22, 32.
24. Li, T. X.; Liu, F.; Teng, G.; Li, N.; Liang, W. T. Paint Coat Ind 2005, 35, 6.
25. Wang, Y. P.; Pei, X. W.; He, X. Y.; Yuan, K. Eur Polym J 2005, 41, 1326.
26. Yu, Z. G.; Zhang, Z. B.; Yuan, Q. L.; Ying, S. K. Adv Polym Technol 2002, 21, 268.
27. Jia, Z. F.; Zhou, J. F.; Zhang, Y. J.; Dang, H. X. Paint Coat Ind 2005, 35, 7.
28. Gao, J. M.; Nie, X. Y.; Fang, R.; Song, Y. H. Paint Coat Ind 2003, 33, 1.
29. Wang, Y. P.; Gao, J. M.; Li, Y. F.; Gu, S. J.; Zhang, F. A. Paint Coat Ind 2005, 35, 17.
30. Spinu, M.; Brennan, A.; Rancourt, J.; Wilkes, G. L.; McGrath, J. E. MRS Symp Proc 1990, 175, 179.
31. Tian, J. MS Dissertation, Hubei University, 2003.
32. Stöber, W.; Fink, A.; Bohn, E. J Colloid Interface Sci 1968, 26, 6269.

33. Fowkes, F. M. Ind Eng Chem 1964, 56, 40.
34. Owens, D. K.; Wendt, R. C. J Appl Polym Sci 1969, 13, 1741.
35. Yang, R.; Liu, Y. J.; Wang, K. H.; Yu, J. J Anal Appl Pyrolysis 2003, 70, 413.
36. Vega-Baudrit, J.; Navarro-Bañón, V.; Vázquez, P.; Martín-Martínez, J. M. Int J of Adhes Adhes 2006, 26, 378.
37. Brinker, C. J.; Scherer, G. W., Eds. The Physics and Chemistry of Sol–Gel Processing; Academic Press: Boston, 1990; p. 581.
38. Chen, Y. J.; Cheng, S. Y.; Wang, Y. F.; Zhang, C. C. J Appl Polym Sci 2006, 99, 107.
39. Duran, A.; Fernandez-Navarro, J. M.; Casariego, P.; Joglar, A. J Non-Cryst Solids 1986, 82, 69.
40. Huang, Z. B.; Tang, F. Q. Acta Polym Sinica 2004, 835.
41. Reculusa, S.; Mingotaud, C.; Bourgeat-Lami, E.; Duguet, E.; Ravaine, S. Nano Lett 2004, 4, 1677.
42. Yang, T. T.; Yao, L.; Peng, H.; Cheng, S. Y.; Park, I. J. J Fluorine Chem 2006, 127, 1105.